ELSEVIER

Journal of Power Sources 94 (2001) 26–35

JOURNAL OF POWER SOURCES

www.elsevier.com/locate/jpowsour

High thermal conductivity negative electrode material for lithium-ion batteries

Hossein Maleki[a,*], J. Robert Selman[b], R.B. Dinwiddie[c], H. Wang[c]

[a]*Motorola Energy System Group (ESG), 1750 Belle Meade Court, Lawrenceville, GA 30043, USA*
[b]*Center for Electrochemical Science and Engineering, IIT, Chicago, IL 60616, USA*
[c]*Oak Ridge National Laboratory, Metals and Ceramics Division, Oak Ridge, TN 37831-6064, USA*

Received 28 August 2000; accepted 1 October 2000

Abstract

Experimental thermophysical property data for composites of electrode and electrolyte materials are needed in order to provide better bases to model and/or design high thermal conductivity Li-ion cells. In this study, we have determined thermal conductivity (k) values for negative electrode (NE) materials made of synthetic graphite of various particle sizes, with varying polyvinylidene difluoride (PVDF) binder and carbon-black (C-Black) contents, using various levels of compression pressure. Experiments were conducted at room temperature (RT), 150 and 200°C. Requirements for designing a high thermal conductivity NE-material are suggested. Detailed statistical data analysis shows that the thermal conductivity of the NE-material most strongly depends on compression pressure, followed by graphite particle size, C-Black content and finally PVDF content. The maximum k-value was achieved for the samples made of the largest graphite particles (75 μm), the smallest C-Black content (5 wt.%) and the highest compression pressure (566 kg cm^{-2}). Increasing the PVDF content from 10 to 15 wt.% increased the k-values by 11–13% only. The k-values of all samples decreased with increasing temperature; at 200°C, the k-values were close to each other irrespective of preparation procedure and/or raw material contents. This most likely is due to the relaxation of contact pressure among the graphite particles because of PVDF melting at 155–160°C.

Keywords: Lithium-ion battery; Thermal conductivity; Thermal diffusivity; Specific heat capacity; Graphite

1. Introduction

The negative electrode (NE) of most commercially available Li-ion cells consists of a copper foil coated with a mixture of carbon, an organic binder such as polyvinylidene difluoride (PVDF) and carbon-black (C-Black). The positive electrode (PE) consists of a mixture of lithium transition metal oxides, PVDF and C-Black coated onto aluminum foil. A micro-porous polymer (separator, Sp) having good ionic conductivity and sufficiently low electronic conductivity separates the PE from the NE. The NE/Sp/PE assembly is flooded by an electrolyte medium consisting of a lithium-salt dissolved in organic solvents.

Abuse conditions (high discharge/charge rates, overcharge, and operation at high ambient temperature) accelerate the net accumulation of heat in Li-ion cells. When the rate of heat generation exceeds that of heat dissipation, the cell may experience ''thermal runaway'' accompanied by internal pressure buildup, which could lead to bursting of the cell and/or fire. Because of these safety issues, battery designers incorporate one or more safety devices such as a current-interrupt, shut-down-separator, vent, rupture-disk or ploywitch in Li-ion cells. In the battery-packs for portable electronics, incorporation of one to three levels of safety circuitry is practiced in order to insure product and customer safety. These safety devices are designed to limit operation of the Li-ion cell to temperatures below 60°C, within upper/lower cut-off voltages of ~2.75 and ~4.2 V, respectively. They may also moderate charge/discharge rates. However helpful, such precautions are costly, and yet little effective once the thermal runaway, for any reason, is initiated inside a Li-ion cell.

Therefore, researchers have been using modeling [1–13] to predict the thermal behavior of Li-ion cells of various designs over a wide range of operating conditions. Several research groups have studied the thermal stability/behavior of Li-ion cells [14–16]. Others investigated the thermal stability/behavior of NE and PE materials and their reaction

* Corresponding author. Tel.: +1-770-338-3146; fax: +1-770-338-3321.
E-mail address: hossein_maleki-g14451@email.mot.com (H. Maleki).

0378-7753/01/$ – see front matter
PII: S0378-7753(00)00661-3

Nomenclature

C_p	effective specific heat capacity (J g^{-1} K^{-1})
k	thermal conductivity (W m^{-1} K^{-1})
m	mass (kg)
t	time (s)
α	thermal diffusivity (m^2 s^{-1})
ρ	effective density (kg m^{-3})
τ	dimensionless time

with electrolyte [17–21]. Most of these published articles deal with the effect of lithiation of NE-material and/or delithiation of PE-material, in combination with the effect of temperature. Overall, however, their conclusion is that the thermal stability of a Li-ion cell could actually decrease with increase in temperature. The rate of heat generation depends primarily on the stage of lithiation of the NE-material and delithiation of the PE-material and on the thermal reactivity of these particular stages with electrolyte. Delithiated PE materials are thermally unstable even at 40°C, however, at 155–170°C they start to decompose vigorously and release oxygen, which reacts with thermally activated electrolyte at a very fast rate. This, in fact, is one of the basic reasons for the lack of success in adding non-flammable and/or heat retarding materials in order to limit the heat generation of Li-ion cells during thermal runaway. In the case of NE-materials, the passivation-layer breaks down near 100–115°C. Then the lithiated NE-material starts slowly reacting with electrolyte, and finally reacts strongly with PVDF as the temperature reaches 230–250°C [22]. Depending on the type of carbon and electrolyte, this reaction may account for the larger part of total heat generation of fully charged Li-ion cells undergo thermally abusive conditions. In our own studies, we found that lithiated NE-material made of graphite has a stronger thermal reaction with selected electrolytes than mesocarbon microfiber NE-material.

The particle sizes of NE and PE materials play an important role in making Li-ion cells of high thermal stability. Smaller particle size tends to increase the rate of heat generation of Li-ion cells under thermally/electrically abusive conditions [23–25]. Types of electrolyte also play an important role in the total amount as well as the rate of heat generation. Very few studies have been conducted on this aspect of Li-ion cell safety. Accelerating rate calorimetry (ARC) results of Hasegawa et al. [26] suggest that exothermic heat development by electrolyte/electrode reaction is due to thermal reactions of the solvents with electrode materials. Using ARC, Richard and Dahn [17] evaluated the thermal stability of lithiated MCMB, of particle sizes of 15 or 25 mm, in electrolyte containing EC:DMC and 1M $LiPF_6$ or $LiBF_4$. Their results indicate that the heat generation increases with an increase in lithiation of MCMB, and that the heat generation due to SEI-layer formation depends on the EC content of the electrolyte. The onset of thermal reaction occurs at lower temperature in the $LiBF_4$ containing electrolyte than in the electrolyte containing $LiPF_6$.

Many methods such as partial oxidation of carbon [27], doping carbon with boron [28] and partial substitution of PVDF with hexafluoro-propene (HFP) [29] have been suggested to decrease the exothermic heat generation of NE-materials of a Li-ion cell. Substitution of carbon-based NE-materials by metallic/intermetallic compounds is being studied. Kepler et al. [30] report the potential application of $Li_xCu_6Sn_5$ ($0 < x < 13$) as NE-material for Li-ion cells. This material's gravimetric energy density (2864 mA h ml^{-1}) is much higher than that of Li_xC_6 (837 mA h ml^{-1}) and it most likely offers a higher thermal stability. Ehrlich et al. [31] investigated Ni–Sb alloys as NE-material candidates for Li-ion cells. They too reported a much higher gravimetric energy density of their material compared to Li_xC_6.

Many models are being developed to predict the thermal stability of Li-ion cells of various chemistries, i.e. electrodes and electrolytes of different chemical stability whose individual component characteristics are known. However, very little experimental information is available on the thermophysical characteristics of composite electrode materials of the type used in Li-ion cells of high thermal conductivity. To develop reliable models, one must use accurate true experimental thermal conductivity data for the cell components, valid under the exact conditions for which the model is developed. Therefore, no accurate estimation of the effective thermal conductivity of an electrode composite system is possible. If, for example, the exact effects of compression pressure on the assumed electrode are not known. For this reason, most model predictions are unreliable, if not incorrect.

This article presents thermal conductivity (k) data for NE-materials made of synthetic graphite of various particle sizes, with varying PVDF binder and C-Black contents, at varying levels of compression pressure: at RT, 150 and 200°C. The k-value was calculated from the product of thermal diffusivity (α), measured using the laser flash thermal diffusivity (LFTD) technique, effective specific heat capacity (C_p) and density of the NE-material samples. Included is information on the procedure for maximizing the thermal conductivity of the NE-material, within the ranges studied in this work. Modeling of the temperature rise in, and heat conduction to/from, a prototype system of four graphite particles surrounded by PVDF/electrolyte medium was used to interpret and confirm the effect of compression pressure on the thermal conductivity of NE composite material.

2. Experimental

2.1. Sample preparations

The NE-materials investigated in this study were disk-shaped pellets (diameter ~1.5 cm, and thickness $9.5 < L < 1.10$ mm) made from synthetic graphite (Lonza

G + T, Switzerland) of particles of 6, 15, 44 or 75 μm, PVDF binder 10 or 15 wt.%, (Kynar-720, elf-atochem, USA) and C-Black 5 or 10 wt.% (Alfa, USA). Samples were prepared at compression pressures of 280, 425 or 566 kg cm^{-2}; thermal conductivity was evaluated at RT, 150 and 200°C for all samples.

NE-material samples were prepared using the following procedure:

1. Dissolve a prescribed mass of PVDF in acetone and heat at 45°C, overnight.
2. Add graphite/C-Black powder in selected mass ratio to the PVDF/acetone solution from step 1, and mix for 20 min using Spex-8000 Mixer/Mill. After mixing, leave the slurry material open in the atmosphere for 4–5 h to allow excess acetone to evaporate. This converts the slurry to a very thick paste.
3. Use stainless steel molding apparatus and CARVER-Press to compress the pastes into pellets. The selected compression pressure (280, 425 or 566 kg cm^{-2}) must be delivered by a three-step process. One third of the final compression pressure is applied at each step, with 5 min intervals between steps. The wait time before application of each compression step insures uniform material distribution in the NE-material pellet.

Graphite and C-Black porosity both were measured using a Micrometric 9320 mercury pore sizer. The surface area of C-Black is 100–125 m^2 g^{-1}. For graphite particles of 6, 15, 44 and 75 μm the surface area values are 17.85, 10.15, 4.93 and 3.02 m^2 g^{-1}, respectively. These values are slightly different than those reported by Kinoshita [32] for SFG-graphite samples of the same particle sizes (15.2, 8.8, 4.2 and 3.5 m^2 g^{-1}).

2.2. Thermal conductivity

If thermal diffusivity (α) values of samples are known, then thermal conductivity (k) can be calculated from the product of α with the effective values of density (ρ) and specific heat capacity (C_p). This indirect method of obtaining thermal conductivity data has proved to be as accurate as, and simpler than, the direct measurement.

2.2.1. Specific heat

The effective C_p was calculated from mass-fraction-weighted values of C_p for each of the existing components in the samples using Eq. (1):

$$C_p = \frac{\sum(mC_p)_i}{\sum(m)_i} \quad (1)$$

Here, m and C_p are the mass fraction and specific heat capacity of the ith component, respectively. The data were acquired from [9].

2.3. Thermal diffusivity

Fig. 1 shows a schematic of the laser flash thermal diffusivity (LFTD) setup used to measure thermal diffusivity of disk-shaped NE-material pellets. The front face of a sample is subjected to a short pulse of a laser (pulse width

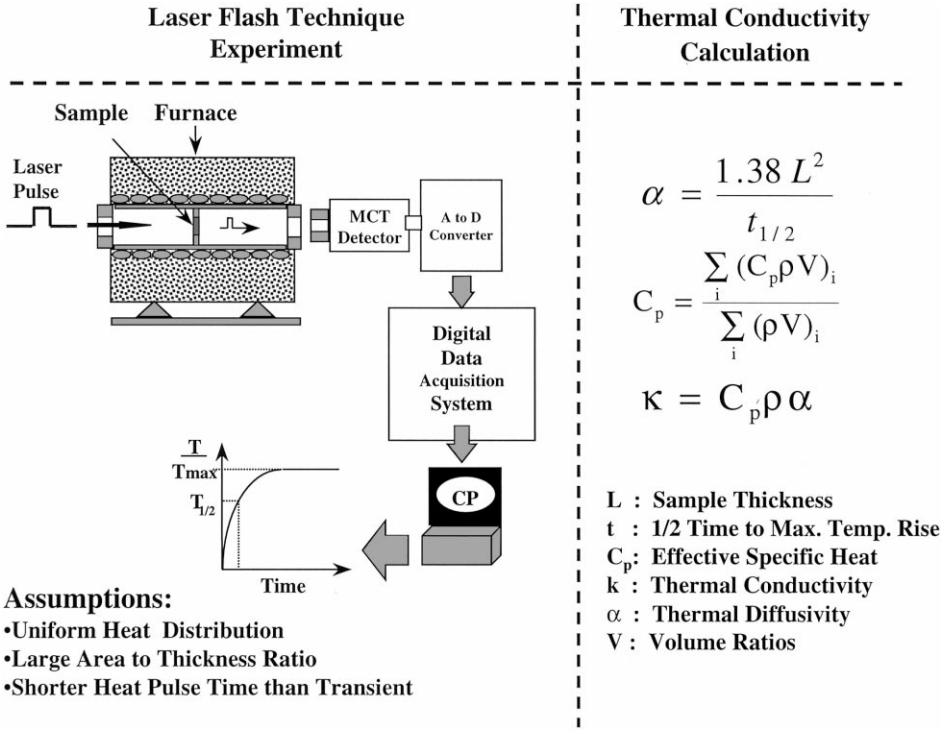

Fig. 1. Schematic of laser flash technique used for measuring thermal diffusivity of NE-material pellets.

is 0.8 ms); and the temperature rise at the rear face of the sample is measured as a function of time by an infrared (IR) detector. Given the sample thickness (L) and the time for the sample rear face to reach half of the maximum temperature rise ($t_{1/2}$), α-values were calculated using the equation,

$$\alpha = \frac{CL^2}{t_{1/2}} \tag{2}$$

where C is a constant: $C = 1.38$ if no heat loss is present during the test. Eq. (2) is an approximate solution of the one-dimensional heat transfer equation [33].

$$\alpha \nabla^2 T = \frac{\partial T}{\partial t} \tag{3}$$

Here, the assumed experimental conditions are: (i) a slab of finite thickness and large area is uniformly illuminated without heat losses, so heat conduction is one-dimensional and the transient temperature is $T(x, t)$; (ii) input energy pulse time much shorter than the time required for that energy to be diffused across the sample and (iii) uniform energy distribution on the front face of the sample. Correction for effects of finite pulse time, non-uniform heating and heat-loss are discussed elsewhere [34–36]. In our experiments, however, samples of high aspect ratios (diameter/thickness) were selected, the input pulse time was less than 1% of the heat diffusion characteristic time and a uniform thermal energy was applied over the front face of the samples. The thermal diffusivity set-up used for this study is described in detail elsewhere [37].

The sample diameter/thickness ratio is critical in obtaining an accurate α-value. If sample thickness is less than optimum, then its rear face temperature rises too rapidly. This causes the IR detector to saturate. If the sample is too thick, then a portion of the input thermal energy, applied to the front face of the sample, will be lost to the surroundings, prior to detection of the temperature raise at the rear face of the sample. Since, the half-maximum temperature-rise time varies with the square of the sample thickness, an accurate measurement of sample thickness is critical. In our case, the density of each sample was calculated based on the volume measured after the thermal diffusivity measurement experiments had been conducted. This was to incorporate any changes in sample geometry due to exposure to input pulse energy and furnace temperature increase from RT to 150 and 200°C during thermal diffusivity measurements.

3. Data analysis

Statistical data analysis software (JMP-Version3) package was used to evaluate overall effects of changing parameters (C-Black and PVDF contents, particle-size, and compression pressure) on thermal conductivity of the NE-material. Fig. 2 is a graphical representation of the effects of changing

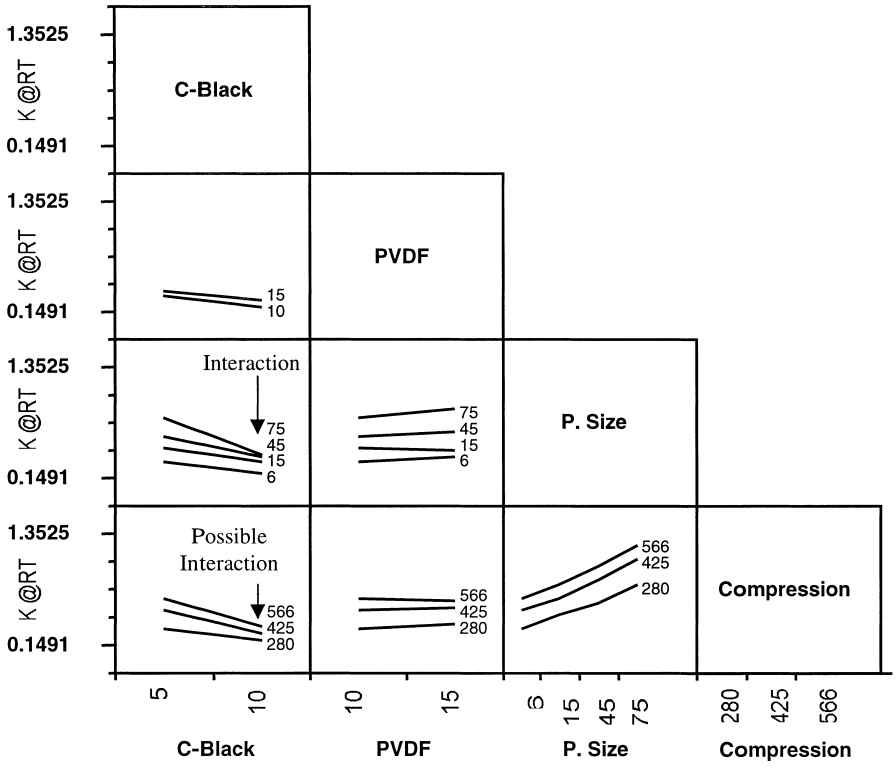

Fig. 2. Effects of changing the parameters (C-Black and PVDF binder contents, particle size and compression pressure) on the thermal conductivity of synthetic graphite NE-material at room temperature. Plots approaching each other, in either end, are indicative of possible interaction of the effects of parameters.

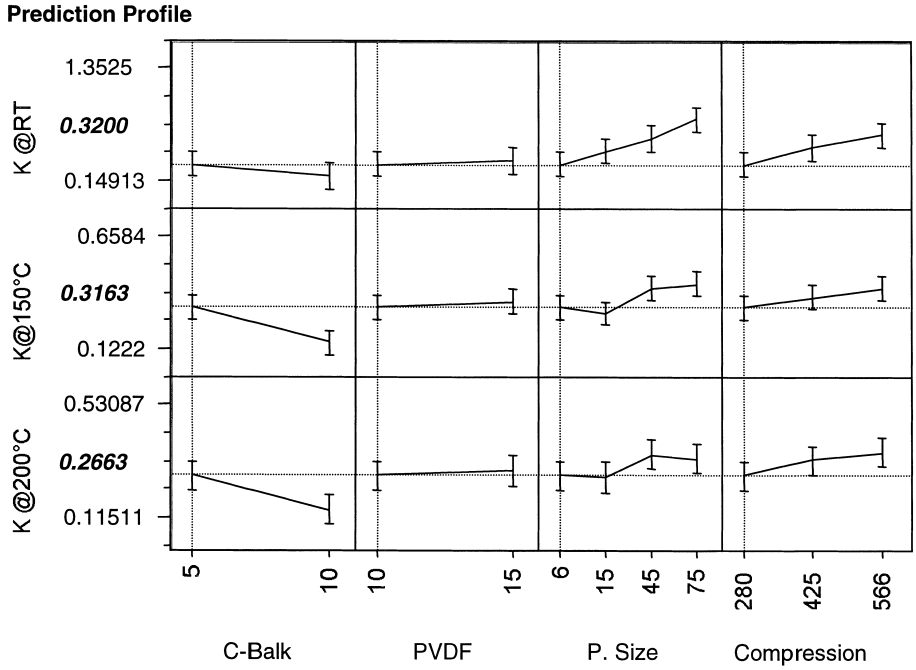

Fig. 3. Thermal conductivity of the baseline NE-material sample at RT, 150 and 200°C vs. C-Black and PVDF contents, particle size and compression pressure with values shown under the cross-hair lines.

the parameters on thermal conductivity of the RT samples. Note that (1) the changes in the slope of each plot can be related to the effects that single-parameter change has on thermal conductivity and (2) plot lines approaching each other, at either end, are indicative of interaction of parameters with each other as they affect thermal conductivity. Fig. 3 is a typical example of composite plots used to evaluate the effects of changing one parameter (e.g. C-Black) on thermal conductivity of the NE-material samples. At various temperatures, while keeping all other parameters constant.

4. Results and discussion

Table 1 gives *k*-values at three different temperatures for NE-materials prepared by changing one of the parameters (C-Black content, PVDF content, particle size, or compression pressure) while keeping all the others constant. The changed parameter for each case is bold italicized. Set-1 rows and column 2 give the parameters used in the case of the baseline sample in which the NE-material was prepared by using the lowest C-Black and PVDF contents, with the smallest graphite particle size and compression pressure. Also included are the highest *k*-values achieved using the lowest C-Black content and the highest PVDF content, particle size and compression pressure.

Table 2 presents a summary of the effect of changing one parameter by itself (e.g. C-Black) and its effect in combination with others (e.g. C-Black × PVDF or C-Black× particle size) in this table. The CF represents ''confidence-factor'' that relates to the effect of changing parameters on thermal conductivity: CF-value <0.05, for a single parameter (e.g. C-Black) is a indicative of a strong effect of changing C-Black content on the thermal conductivity. In the case of a two-parameter effect (e.g. C-Black × PVDF), CF-values <0.05 show strong interaction of effects due to both parameters on each other and, together, on thermal conductivity.

4.1. Baseline sample

Fig. 3 shows composite plots of thermal conductivity versus various parameters. The cross-hair line represents C-Black 5 wt.%, PVDF 10 wt.%, graphite particle 6 μm and compression pressure 280 kg cm^{-2}, used in making of ''baseline'' sample. This combination provided a NE-material with *k*-value of 0.3200 W m^{-1} K at RT, and 0.3162 and 0.2663 W m^{-1} K when the same sample was tested at 150 and 200°C, respectively.

4.2. Effect of carbon-black content

When the C-Black content was increased from 5 to 10 wt.% and all others parameters kept as they were in the baseline sample, the *k*-values decreased to 0.1919, 0.1473 and 0.1407 W m^{-1} K for the sample tested at RT, 150 and 200°C, respectively. This decrease of thermal conductivity values, compared to that of the baseline sample, may mostly be attributed to the high surface area of C-Black, which also increases the surface area of the bulk sample. For example, increasing the C-Black content from 5 to 10 wt.% translates in a 18–20% increase in surface area of

Table 1
Thermal conductivity (k) values of NE-material made of synthetic graphite of various particle size, C-Black and PVDF contents and compression pressure[a]

Parameters	Values	Thermal conductivity, k at different temperatures		
		RT	150°C	200°C
C-Black	5			
PVDF	10			
Particle size	6	*0.3200*	*0.3163*	*0.2663*
Compression	255			
C-Black	***10***	0.191	0.147	0.1407
PVDF	10			
Particle size	6			
Compression	255			
C-Black	5			
PVDF	***15***	0.365	0.345	0.2859
Particle size	6			
Compression	255			
C-Black	5			
PVDF	10			
Particle size	***15***	0.465	0.289	0.2619
Compression	255			
C-Black	5			
PVDF	10			
Particle size	***44***	0.599	0.410	0.344
Compression	255			
C-Black	5			
PVDF	10			
Particle size	***75***	0.798	0.431	0.329
Compression	255			
C-Black	5			
PVDF	10			
Particle size	6			
Compression	***425***	0.505	0.366	0.3261
C-Black	5			
PVDF	10			
Particle size	6			
Compression	***566***	0.632	0.408	0.354
Parameters used to design high thermal conductivity negative electrode				
C-Black	5			
PVDF	15	*1.2511*	*0.6036*	*0.4882*
Particle size	75			
Compression	566			

[a] The numbers indicated in bold italicized font are values changed from that of baseline sample with parameters shown in column 2, row 2.

the NE-material of the 6 μm graphite particles. It is a well-known fact that high surface area generates heat-trap-centers inside the sample and consequently lowers its heat transfer rate.

Similar statistical data analysis as in Fig. 3, showed that for all three temperatures changing the C-Black content causes particle size effects on thermal conductivity to change significantly, yet the effects of compression pressure or PVDF contents remain unchanged. This suggests that the effect of changing the C-Black content interacts with effects of changing the particle size (item 5, CF-values <0.05), but not with the effect of PVDF content (item 3, CF-values >0.05). The effect of C-Black content interacts slightly with that of compression pressure effects at RT (item 8, CF = 0.0406), but not at all with those at 150 and 200°C (item 8, CF-values >0.05). The overall results suggest that high thermal conductivity NE-material can be made by a correct combination of C-Black content with carbon particle size. Effects of compression or PVDF content are largely independent of changing O-Black content.

4.3. Effect of PVDF content

In case where the PVDF content was increased from 10 to 15 wt.% and all others parameters kept as they were in the baseline sample, the k-values obtained were 0.3652, 0.3453 and 0.2859 W m^{-1} K at RT and 150 and 200°C, respectively. These values are slightly higher than the k-values for the baseline sample, tested at the same temperature. Statistical analysis show that increasing the PVDF content changes the particle size effect on thermal conductivity at 150 and 200°C, but not at RT. Results indicate no interaction between the effect of PVDF content and that particle size, C-Black content or compression force: in all cases the CF-values > 0.05. The PVDF content effect interacted with the effect of particle size at 150 and 200°C, with CF-values 0.0086 and 0.0040, respectively (see item 6 in Table 2).

The interaction between the effects of PVDF and particle size at 150 and 200°C may be attributed largely to softening (84°C) and/or melting of PVDF (155–160°C). It is likely that when the PVDF melts, the contact points due to compression among the graphite particles are relaxed, and perhaps some molten PVDF partially covers the surface of the graphite particles. Note that the thermal conductivity of PVDF (0.17 W m^{-1} K) is lower than that of graphite (7–110 W m^{-1} K). These conditions could cause the effects of PVDF and particle size to interact and together change thermal conductivity, at temperatures near/above the melting point PVDF. The overall results, however, suggest that the small decrease in thermal conductivity, due to PVDF content, occurs at high temperature where most Li-ion cells are in need of improved thermal conductivity.

4.4. Effect of particle size

When the graphite particle size was increased from 6 to 75 μm and other parameters kept as they were in the baseline sample, the k-values increased significantly. Fig. 4 shows thermal conductivity versus particle size at RT, 150 and 200°C. Thermal conductivity clearly increases with increase in particle size. This may be ascribed to the dominant role that particle size plays in controlling the porosity of a system of particles. Systems containing large particles tend to have a lower porosity than systems made of small particles. As noted above, high porosity impedes the heat transfer capability of a system of particles. Fig. 4 also shows that the thermal conductivity of the sample decreases

Table 2
C-Black and PVDF contents, graphite particle size and compression pressure effects on thermal conductivity k (W m^{-1} K^{-1}) of NE-material samples[a]

	Source	Confidence-factor, CF			Factors and factors interaction at @ RT, 150, 200°C
		RT	150°C	200°C	
1	C-Black	<0.0001	<0.0001	<0.0001	Strong effects
2	PVDF	0.3290	0.4026	0.6598	No effects
3	C-Black × PVDF	0.5489	0.2808	0.4139	No effects
4	Particle size	<0.0001	<0.0001	<0.0001	Strong effects
5	Particle size × C-Black	0.0050	0.0007	0.0020	Strong effects
6	Particle size × PVDF	0.4516	0.0086	0.0040	Strong effects[b]
7	Compression	<0.0001	<0.0001	<0.0001	Strong effects
8	Compression × C-Black	0.0406	0.3663	0.2918	No effects[b]
9	Compression × PVDF	0.6915	0.3682	0.5532	No effects
10	Compression × particle size	0.8655	0.8040	0.9114	No effects

[a] Single parameters (CF-value <0.05) shows strong effects on thermal conductivity. Double parameters (CF-value <0.05) show strong interaction among both parameters and effects on thermal conductivity.
[b] Only at 150 and 200°C.

with increase in temperature, which tends to weaken the positive effect of particle size increase on thermal conductivity.

Statistical data analysis showed presence of no interactions between the effects of particle size and PVDF content at RT, and weak interactions at 150 and 200°C (item 6: CF-values are 0.4516, 0.0086 and 0.0040, respectively). This interaction, again, could be attributed to softening and melting of the PVDF because of temperature increase to 150 and 200°C. The particle size effect also interacts with the effect of C-Black contents. For this interaction, the CF-values are 0.005, 0.0007 and 0.002 for the sample tested at RT, 150, and 200°C, respectively (see item 5 in Table 2). Overall, this suggests that to obtain electrodes of stable thermal conductivity, one should consider combinations of filler and binder material with no and/or minimal interaction effects at high temperature. For Li-ion battery electrodes, this simply means selection of electrode materials that maintain their RT properties at temperatures above ∼140°C.

4.5. Effect of compression

When the compression pressure was increased from 255 to 566 kg cm^{-2} and all other parameters kept as they were in the baseline sample, the k-values of the sample increased over those of the baseline sample at RT, 150 and 200°C. Fig. 5 shows thermal conductivity values vs. compression pressure at RT, 150 and 200°C. The thermal conductivity of the sample increases with increase in compression pressure, but the effect weakens as the temperature is increased to 200°C. Evidently, the built-up compression of the graphite particle relaxes as the PVDF softens and melts, once the temperature increases to 150 and 200°C. The overall effects of compression pressure on thermal conductivity, however, appeared to be of the same order as that of particle size, however, the compression effect is less affected by increase in temperature between 150 and 200°C.

Statistical data analysis shows that the only possible interaction of the effect of compression with other variables

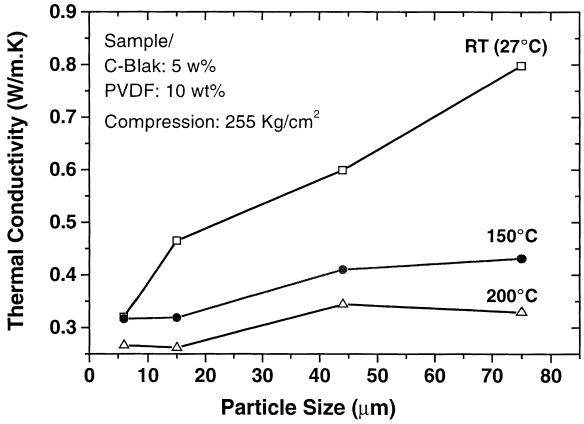

Fig. 4. Thermal conductivity of NE-material at RT, 150 and 200°C vs. particle size. Other parameters were as in the baseline sample.

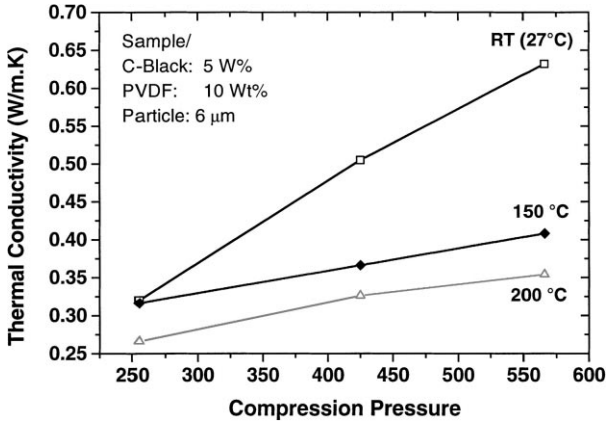

Fig. 5. Thermal conductivity NE material at RT, 150 and 200°C vs. compression pressure. Other parameters were as in the baseline sample.

is the interaction with the effect of C-Black content at RT (see item 8 in Table 2). Other parameters are not affected by changing the compression pressure. This suggests that the compression pressure, within the range selected here, should be adjusted mostly based on the C-Black content, not on the PVDF content or graphite particle size. In an actual electrode manufacturing process, cylindrical rollers of different diameters can supply various linear calandering pressures (kg m^{-1}). This could provide a wider range of compression options, which can be used to obtain electrodes of optimum thermal conductivity.

4.6. High thermal conductivity NE-material

When using C-Black and PVDF contents of 5 and 15 wt.%, respectively, graphite particle size 75 μm, and compression pressure 565 kg cm^{-2}, the sample thermal conductivity was found to be 1.2510, 0.6036 and 0.4882 W m^{-1} K at RT, 150 and 200°C, respectively. These are the highest *k*-values we achieved, using minimum C-Black content, combined with highest PVDF content and graphite particle size, and highest compression pressure.

High thermal conductivity NE-material may play an important role in obtaining Li-ion cells of high thermal stability. This issue is even more important for the high capacity/power density cells considered in EV applications. Low thermal conductivity NE-materials tend to maintain heat in itself, rather than passing it on to the electrolyte/separator medium, which in fact has a relatively higher heat capacity and could accommodate more heat than the NE-material. High heat accumulation in electrodes becomes problematic especially for large Li-ion cells operated at, or exposed to, temperatures higher than 60°C. This always could increase the chance of hot spots in electrodes.

From the perspective of battery design, the PVDF and C-Black contents offer very little room for change to alleviate safety problem of Li-ion cells. Increased PVDF content increases the thermal conductivity of the NE-material very little, and also increases the total heat of reaction with Li_xC_6, in case of thermal runaway. Increased C-Black content improves the adhesion of carbon particles to each other and to the current collector, but it lowers the thermal conductivity and the reversible lithiation capacity of the NE. Hence, changing the particle size and compression pressure offer a wider range of opportunity to design high thermal conductivity NE-materials.

The C-Black content in PE-material should be studied even more carefully, since, a higher concentration of C-Black is needed to elevate the thermo-electrical conductivity of the PE in Li-ion cells.

5. Thermal modeling

As noted above, the thermal conductivity of NE-material is most strongly affected by the compression pressure used in pressing of the sample-slurry to desired density. To prove this, a modeling approach is used to determine the relative temperature rise and distribution in an idealized unit of NE-material of a low and a high compression (LC and HC) pressure. The sample unit consists of four graphite particles (length 44 μm and thickness 4 μm) surrounded by an electrolyte/PVDF medium. In the LC case, the graphite particles are spaced 4 μm from each other, in both *x* and *y* directions; in the HC case, the graphite particles are 2 μm from each other, again in both *x* and *y* directions. The distance between edges of the particles and the edges of the unit is set at half of the distance between the particles, in the same

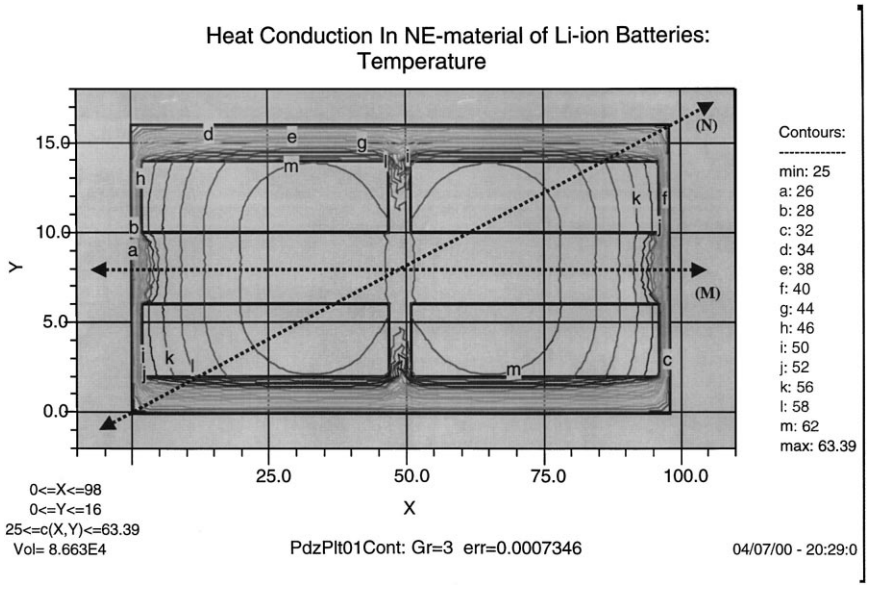

Fig. 6. Simulated isothermal contours of temperature distribution in NE-material unit considered using compression pressure that force graphite particles at net distance of 4 μm from each other. The particles surrounding medium is considered field with PVDF and electrolyte.

units: for LC and HC sample the distances are 2 and 1 μm, respectively.

In this model, each particle is considered as a source that supplies continuous power to heat itself and the surrounding particles and PVDF/electrolyte medium. Heat transfer is only by conduction, no convection heat transfer is considered because in an actual Li-ion cell the electrolyte is not mobile. The same initial and boundary conditions were applied to both of the LC and HC samples units. Effective thermal conductivity of graphite and PVDF/electrolyte medium were considered to be 57 and 1 W m^{-1} K, respectively; the initial temperature was 30°C; and heat generation considered was 10 W m^{-3}. This model is intended to show the effect of compression pressure on the temperature rise and distribution in NE-material based on the assumed conditions here. It does not predict the rate of heat transfer from a NE-material in an actual Li-ion cell, but only estimates the effect of compression on the heat transfer relative to the selected case here.

Fig. 6 shows the isothermal contours of temperature distribution in the LC-sample. Similar modeling was conducted for the HC-sample (figure not included). Fig. 7(a) and (b) show the temperature rise and distribution along M and N lines in both the LC and HC samples. The results indicate that the overall temperature, in relative terms, of the HC sample remains lower than that for the LC-sample by ∼27%. In a sense this agrees with the data given in Table 1, which show that thermal conductivity of sample increases with increasing compression force.

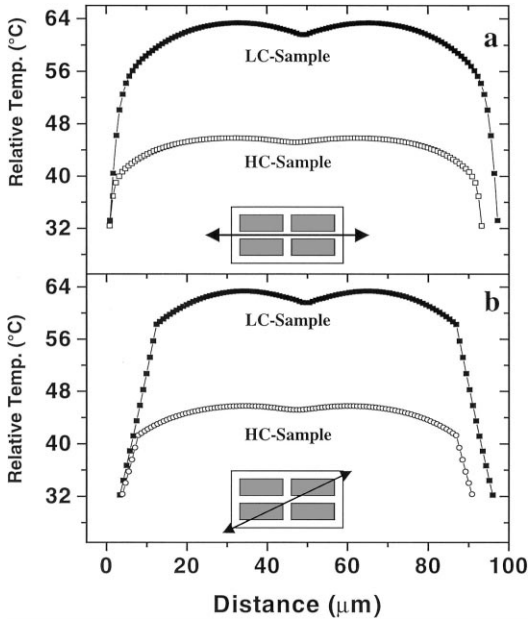

Fig. 7. Temperature distribution over the NE-materials of low and high compression (LC and HC) units, containing four-graphite particles surrounded by PVDF and electrolyte: (a) temperature rise along diagonal line noted as "N"; (b) temperature rise along horizontal line extended through the middle of the particles noted as "M".

6. Conclusion

Thermophysical property data for PE, NE and electrolyte composite materials are needed in order to develop reliable models to predict thermal behavior of Li-ion cells. This investigation was focused on the thermal conductivity of NE-materials which consist of synthetic graphite of various particle sizes, varying PVDF binder and C-Black contents, compacted under various compression pressures. In addition, the effect of temperature on thermal conductivity was investigated. The thermal conductivity of NE-materials was found to increase with increasing compression pressure, graphite particle size, PVDF binder content and to decrease with increasing C-Black content. Thermal conductivity decreases with increasing temperature. Among the various factors, PVDF has the least effect on the thermal conductivity. Particle size and compression pressure appear to play the most important role in making a high thermal conductivity composite NE. A simple thermal modeling approach proved information on the importance of compression pressure effects on making high thermal conductivity NE composite.

Based on these studies, a NE-material of optimum thermal conductivity is achieved by using the lowest C-Black content, the highest possible compression pressure and finally the largest particle size. However, because of strong exothermic reaction between the lithiated NE-material and PVDF, and lowering of the reversible lithiation capacity with increasing C-Black content, particle size and compression pressure offer the best options in designing a high thermal conductivity composite NE.

Acknowledgements

Authors thank Miss Lora Woods and the mechanical-design technical staffs of Illinois Institute of Technology (IIT) for providing us with material pore-size analyzer equipment and molding-apparatus for making NE-material samples pellets, and Said Al-Hallaj contributions in thermal modelling. This work was supported *in part* by the Assistant Secretary of Energy Efficiency and Renewable Energy as part of the HTML User Program at ORNL managed by the UT-Battelle, LLC, for the DOE, Contract No. DE-AC05-00OR22725.

References

[1] L. Rao, J. Newman, J. Electrochem. Soc. 144 (1997) 2697.
[2] Y. Chen, J.W. Evans, J. Electrochem. Soc. 140 (1993) 1833.
[3] Y. Chen, J.W. Evans, J. Electrochem. Soc. 141 (1994) 2947.
[4] Y. Chen, J.W. Evans, J. Electrochem. Soc. 143 (1996) 2708.
[5] D. Bernardi, E. Pawlikowski, J. Newman, J. Electrochem. Soc. 132 (1985) 15.
[6] C.R. Pals, J. Newman, J. Electrochem. Soc. 142 (1995) 3274.
[7] C.R. Pals, J. Newman, J. Electrochem. Soc. 142 (1995) 3282.
[8] J. Newman, W. Tiedemann, J. Electrochem. Soc. 142 (1995) 1054.

[9] K. Kanari, K. Takano, Y. Saito, Bull. Electrochem. Lab. 60 (1996) 65.
[10] Y.I. Cho, G. Halpert, J. Power Sources 18 (1986) 106.
[11] B. Tsenter, M. Golod, EE AES System Magazine 23 (9) (1998).
[12] F.B. Tudron, J. Electrochem. Soc. 128 (1988) 516.
[13] F.B. Tudron, Electrochem. Soc. Proc. 94 (28) (1995) 165.
[14] T.D. Tran, J.H. Feikert, R.W. Pekala, K. Kinoshital, J. Appl. Electrochem. 26 (1996) 1161.
[15] J.S. Hong, H. Maleki, S. Al-Hallaj, L. Redy, J.R. Selman, J. Electrochem. Soc. 145 (1998) 1489.
[16] L. Song, Y. Chen, J.W. Evans, J. Electrochem. Soc. 145 (1997) 3797.
[17] M.N. Richard, J.R. Dahn, J. Electrochem. Soc. 146 (1999) 2069.
[18] D. Aurbach, M.D. Levi, E. Levi, B. Markovsky, G. Salitra, H. Teller, in: C.F. Holmes, A.R. Landgrebe (Eds.), Batteries for Portable Applications and Electric Vehicles, Electrochem. Soc. Proc. Series, Vol. 97-18, 1997, p. 941.
[19] D. Aurbach, Y. Ein-Eli, O. Chusid, Y. Carmeli, M. Bakai, H. Hamin, J. Electrochem. Soc. 141 (1994) 603.
[20] U. von Sacken, E. Nodwell, A. Sundher, J.R. Dahn, J. Power Sources 54 (1995) 240.
[21] J.R. Dahn, E.W. Fuller, M. Obrovac, U. von Sacken, J. Solid State Ionic 69 (1994) 12.
[22] H. Maleki, G. Deng, A. Anani, J. Howard, J. Electrochem. Soc. 146 (1999) 3224.
[23] U. von Sacken, E. Nodwell, A. Sundher, J.R. Dahn, J. Power Sources 54 (1995) 240.
[24] M.W. Juzkow, S. Mayer, in: Proceedings of the Twelfth Annual Battery Conference on Applications and Advances, I-IEEE, New York, 1997, p. 181.
[25] W.LiJ.C. Currie, J. Wolstenholme, J. Power Sources 68 (1997) 565.
[26] K. Hasegawa, Y. Arakawa, J. Power Sources 43/44 (1993) 523.
[27] C. Menachem, D. Golodnitssky, E. Peled, Electrochem. Soc. Proc. 138 (1995) 157.
[28] B.M. Bay, J.R. Dahn, Electrochem. Soc. Proc. 141 (1994) 907.
[29] D. Pasquier, F. Disma, T. Bowmer, A.S. Gozdaz, G. Amatucci, J.-M. Tarascon, J. Electrochem. Soc. 145 (1998) 472.
[30] K.D. Kepler, T. Vaughey, M.M. Thackeray, Electrochem. Soild State Lett. 2 (1997) 307.
[31] G.M. Ehrlich, C. Durand, X. Chen, T.A. Hugener, F. Spiess, S.L. Suib, J. Electrochem. Soc. 147 (2000) 886.
[32] T.D. Tran, J.H. Feikert, X. Song, K. Knoshita, J. Electrochem. Soc. 142 (1995) 3297.
[33] R.E. Taylor, K.D. Maglic, in: K.D. Maglic A. Cezairliyan, V.E. Peletsky (Eds.), Compendium of Thermophysical Property Measurement Methods: Survey of Technique, Plenum Press, New York, 1984, 305 pp.
[34] L.M. Clark III, R.E. Taylor, J. Appl. Phys. 46 (1975) 714.
[35] M.I. Darby, S.D. Preston, G. Whitaker, Analysis of diffusivity measurements on four-layer samples, J. Appl. Phys. 21 (1988) 1146.
[36] R.F. Bulmer, R. Taylor, Measurement by the flash method of thermal diffusivity in two-layer composite sample, High Temperatures High Pressures 6 (1974) 491.
[37] H. Wang, R.B. Dinwiddie, P.S. Gaal, in: K.E. Wilkes, R.B. Dinwiddie, R.S. Graves (Eds.), Multiple Station Thermal Diffusivity Instrument, Technomic Publishing Co., 1996, p. 119.